Available online at www.pelagiaresearchlibrary.com

Pelagia Research Library

Advances in Applied Science Research, 2019, 9(2):1-16

ISSN : 0976-8610
CODEN (USA): AASRFC

The Role of *Arctium lappa* L. Extract against Zinc Oxide Nanoparticles Induced Hepato-Cardiotoxicity and Hyperlipidemia in Male Rats

Nema A Mohamed[1]*, Heba M Abdou[1], Rasha S S Eldeen[2] and Sabreen S Mohammed[3]

[1]*Department of Zoology, Faculty of Science, Alexandria University, Alexandria, Egypt*
[2]*Department of Medical Biophysics, Medical Research Institute, Alexandria University, Egypt*
[3]*Department of Zoology, Faculty of Science, Omar Al-Mokhtar University, Libya*

ABSTRACT

The present study investigated the potential role of Arctium lappa L. extract against the hepato-cardio toxicity and hyperlipidemia induced by ZnO-NPs in male rats. The groups of this study were Control, ZnO-NPs (50 mg/kg b.w.), ZnO-NPs+Arctium lappa L. (300 mg/kg b.w.) and Arctium lappa L. group. The oral administration of ZnO-NPs caused significant decrease in RBC, Hb, Hct and platelets while, WBC was increased. Liver enzymes and total bilirubin were significantly increased after ZnO-NPs supplementation. On the other hand, protein, albumin and globulin were significantly decreased in ZnO-NPs group. Lipid profile determination revealed hyperlipidemia state in the ZnO-NPs group. The ZnO-NPs group exhibited an oxidative stress as documented by an increase in TBARS and a decrease in GSH and total thiol. CK-MB, PON1, Fe^{+3} were significantly decreased while; LDH, TNF-α, p53, IL-6, Zn^{+2} and Ca^{+2} were increased in ZnO-NPs treated group. In addition, ZnO-NPs caused histopathological changes in liver and heart tissues. In contrast, Arctium lappa L. administration improved the most measured parameters by its antioxidant and anti-inflammatory effects against the ZnO-NPs toxicities.

Keywords: Zinc oxide nanoparticles, *Arctium lappa* L., Liver, Heart, Hyperlipidemia, Oxidative stress, Rats

INTRODUCTION

There has been an exponential increase in using nanoparticles (NPs) due to their wide range of biomedical applications [1]. ZnO-NPs are being investigated for their potential use as fungicides, antimicrobial and as anticancer drugs [2]. ZnO-NPs also used in dyes, paints, rubber, alloys, ceramics, chemical fibers, electronics, catalyst, sunscreens, medical diagnosis, cosmetics, personal care products and food additives [3].

It is agreeable that NP toxicity depends on particle size, shape, surface charge and chemistry, composition, and its subsequent stability. NP cytotoxicity may be related to oxidative stress and pro-inflammatory activity [4]. NPs can enter the human body through different routes and can be distributed throughout the body and taken up by cells through phagocytic or endocytic mechanisms [5,6].

Arctium lappa L. (Burdock, Compositae family) is an edible perennial herb in traditional Chinese medicine and therapies in Europe, North America, and Asia. Burdock is rich in antioxidant agents, such as tannin, gallic acid, arctigenin, quercetin and caffeoylquinic acid. Besides, it is good in treating pharyngitis as it can moisten lung for removing phlegm and wound healing and cures measles. In addition, arctigenin was first found with the ability of effectively improving memory impairment in mice [7].

The present study aimed to investigate the protective role of *Arctium lappa* L. extract against the hepato-cardiotoxicity and hyperlipidemia induced by ZnO-NPs.

MATERIALS AND METHODS

Chemicals

Zinc oxide nanoparticles (ZnO-NPs) and *Arctium lappa* L. (Burdock) were purchased from Sigma-Aldrich Chemical Co. (St. Louis, MO, USA).

Experimental animals

Twenty-eight adult male *Wistar* albino rats (160-170 g) were obtained from Faculty of Agriculture, Alexandria University, Alexandria, Egypt. Rats were housed in a stainless steel wire cage placed in a well-ventilated animal house. They were kept on the basal diet and tap water *ad libitum* and maintained at 25 ± 1°C with 12 h dark and light cycle. The design of the experiments and the protocols were carried out according to the guidelines of the National Institutes of Health (NIH).

Experimental design

Rats were randomly divided into four equal groups, each consisting of seven rats as follows:

Group I

Control group: rats of this group were orally received saline as a vehicle by gavage, daily for 28 days.

Group II

Zinc oxide nanoparticles-treated group (ZnO-NPs): rats of this group were orally received ZnO-NPs alone by gavage at a dose 50 mg/kg body weight dissolved in saline daily for 28 days [8].

Group III

Arctium lappa L. and ZnO-NPs-treated group: rats of this group were orally received *Arctium lappa* L. at a dose of 300 mg/kg body weight [9] and after 15 min. they orally received ZnO-NPs at a dose 50 mg/kg body weight daily for 28 days.

Group IV

Arctium lappa L. treated group: rats of this group were orally received *Arctium lappa* L. alone at a dose of 300 mg/kg body weight dissolved in saline.

Blood samples

At the end of the experimental period, the rats were anesthetized with diethyl ether and sacrificed. Blood was taken by the heart puncture using sterile syringe. The blood samples were placed in weatherman tubes containing EDTA for hematological parameters. The non-heparinized blood was centrifuged at 4000 rpm for 10 min and the serum was collected and stored for the biochemical parameters determination.

Tissue preparation

The liver and heart tissues were immediately isolated from the rats after scarification and washed with cold saline solution. Pieces of liver and heart tissues were taken in 10% formalin for the histological studies.

0.5 g from liver and heart tissues was homogenized in 4.5 ml 0.1 M potassium phosphate buffer (pH:7) using a polytron (Tekmar model TR-10, West Germany). The homogenates were centrifuged at 12000 rpm using cooling centrifuge (Hettich Mikro 220R, Germany) and the supernatant stored at -20°C till used for assaying the other parameters.

Characterization of ZnONPs

X-ray diffraction (XRD) of ZnONPs

The crystallinity was determined by XRD powder diffraction. Analysis was performed by using an XRD SHIMADZU 6000 diffractometer equipped with a Cukα (K=1.54 A°) source, maintaining applied voltage of 40 kV and current at 30 mA. About 0.3 g of dried ZnO-NPs was deposited as a randomly oriented powder into a plexiglass sample container and the XRD patterns were recorded between 5° and 50° angles, with a speed of 5.0°/min. The crystalline domain Diameter (D) was obtained from XRD peaks using the following Scherrer's equation $D=K * \lambda/\beta*\cos\theta$, where

λ is the wavelength of the incident X-ray beam; Θ the Bragg's diffraction angle; β the width of the X-ray pattern line at half peak–height in radian and the dimensionless shape factor (K) has a typical value of 0.89, but varies with the actual shape of the crystalline [10].

Fourier transform infrared spectroscopy (FTIR) of ZnO-NPs

Fourier-Transform Infrared Spectroscopy (FTIR) is an effective method to reveal the composition of products. An FTIR spectrometer simultaneously collects high-spectral-resolution data over a wide spectral range. This confers a significant advantage over a dispersive spectrometer, which measures intensity over a narrow range of wavelengths at a time.

Transmission electron microscopy (TEM) of ZnO-NPs

The size distribution of ZnO-NPs in suspension was measured using a sub micrometer particle size analyzer (Nicomp, Port Richey, FL) and was confirmed to be within the designated range. Images of NP in the vehicle were also obtained by TEM (JEM-2010, JEOL, Tokyo, Japan).

Determination of hematological parameters

The hematological parameters, including RBCs, Hb, Hct, WBCs and PLt were estimated by Particle Counter (ERMA Inc., Tokyo. Model PCE-210).

Biochemical parameters

Determination of liver and heart enzyme activities

The activities of AST (EC: 2.6.1.1) and ALT (EC: 2.6.1.2) were measured according to the method of Bergmeyer et al. [11]. GGT (EC: 2.3.2.2) was estimated by the method of Szasz [12]. The method of Deutsche [13] was used in the determination of lactate dehydrogenase (LDH; E.C.1.1.1.27). The Creatine Kinase (CK-MB) (EC: 2.7.3.2) level in the heart was assayed according to the method of the International Federation for Clinical Chemistry [14]. The activities of the paraoxonase (PON1) enzyme (EC 3.1.1.2) were assayed according to the method of Mueller et al. [15].

Estimation of the liver indices

A colorimetric method of Jendrassik and Grof [16] was used for the determination of total bilirubin levels. Total protein and albumin concentration in serum were assayed by the method of Lowry et al. [17] and Doumas et al. [18], respectively. Serum globulin was calculated according to this equation:

Total protein-albumin=globulin (g/dl)

Lipid profile assay

The total cholesterol [19], LDL-C [20] and HDL-C [21] levels were determined. The serum triglyceride level was determined by the colorimetric method using available commercial kits (Biodiagnostic, Egypt) according to the method described by Bucolo and David [22]. VLDL was estimated according to the equation VLDL=TG/5.

Determination of oxidative stress markers

Lipid peroxidation was measured as thiobarbituric acid-reactive substances (TBARS) in tissues by the method of Tappel and Zalkin [23]. GSH and total thiol contents were estimated by using the methods of Jollow et al. [24] and Sedlak and Lindsay [25], respectively.

Assay of proinflammatory cytokines

Quantitative measurement of rat IL-6 in tissue homogenates according to the method of Ferguson-Smith et al. [26] was estimated. Tumor Necrosis Factor alpha (TNF-α) was estimated by using Enzyme-Linked Immunosorbent Assay kit according to the method of Hedayati et al. [27]. The tumor suppressor (p53), acts primarily as a transcriptional activator that controls the expression of many genes, was estimated by the method of Yang et al. [28].

Determination of some ions

Zn^{+2}, Ca^{+2} and Fe^{+2} levels were performed by atomic absorption analysis using Perkin-Elmer 2380 spectophotometer.

Histopathological studies of liver and heart

Histopathological examination was carried out according to Drury et al. [29]. The excised liver and heart specimens were isolated and immediately fixed in 10% formalin, then treated with conventional grade of alcohol and xylol and

then paraffin embedded. Paraffin blocks were sectioned into 4-5 µm thick sections. The sections were stained with Haematoxylin and Eosin (H & E) stain for studying the histopathological changes.

Statistical analysis

Statistical analyses were performed using the SPSS package for Windows version 22.0. Data were expressed as mean ± S.E. One-way ANOVA was used to analyze differences among groups. Differences between groups were considered statistically significant at $P \leq 0.05$.

RESULTS

Transmission electron microscopy (TEM) of ZnO-NPs

Figure 1 shows the TEM images and selected area electron diffraction patterns of ZnO-NPs annealed at 700°C and 900°C. This image reveals that the product consists of spherical particles with the average size of<100 nm. The Selected Area Electron Diffraction (SAED) shows the crystalline structure, complexity for variable calcination. It indicates that ZnO-NPs are not single crystals, rather are the aggregation of several single crystals (Figure 1).

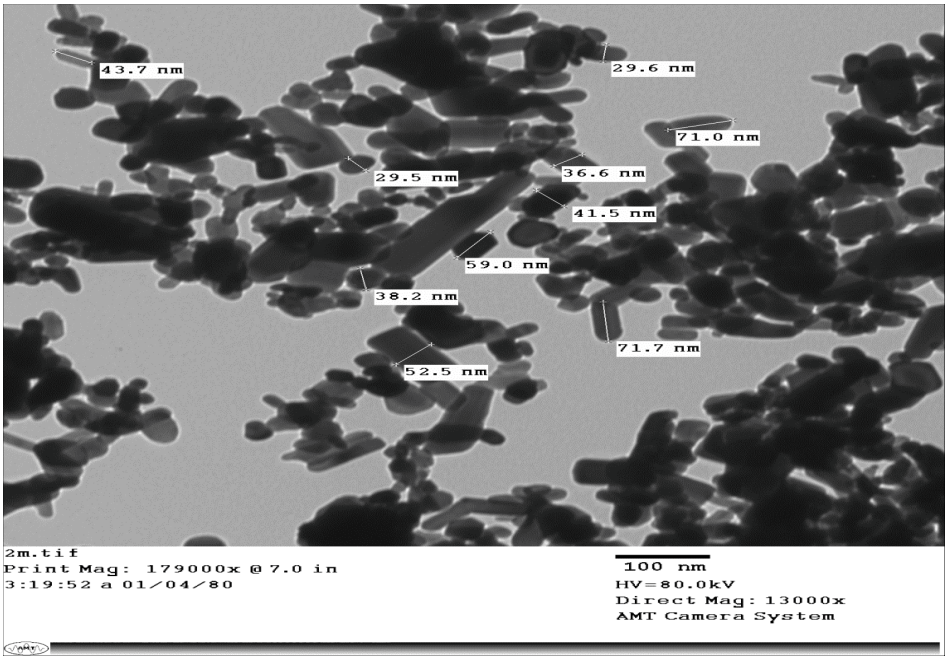

Figure 1: Transmission Electron Microscopy (TEM) of ZnONPs

X-ray diffraction (XRD) of ZnO-NPs

Diffraction lines of ZnO were broadened and diffraction broadening was found dependent on Miller indices of the corresponding sets of crystal planes. For most samples the diffraction line 4000 is narrower than the line 8000 and 8000 is narrower than the line 5000. The average crystallite size of samples S2 (700°C) and S3 (900°C) were determined by the Debye-Scherer formula 0.9 λ/Bcos (θ) and were found to be 26.74 nm and 28.93 nm, respectively. Comparing the XRD report of three samples it has been concluded that the samples calcined at 700°C and 900°C gives a high intensity fine peaks, which can be used for further characterization (Figure 2).

Fourier transform infrared spectroscopy (FTIR) of ZnO-NPs

Figure 3 is a typical FTIR spectrum of pure ZnO nanoparticles, the peak at 417.52 cm^{-1} is the characteristic absorption of Zn-O bond and the broad absorption peak at 3438 cm^{-1} can be attributed to the characteristic absorption of hydroxyl. Anyhow, the FTIR and XRD results showed high purity of the obtained ZnO nanoparticles.

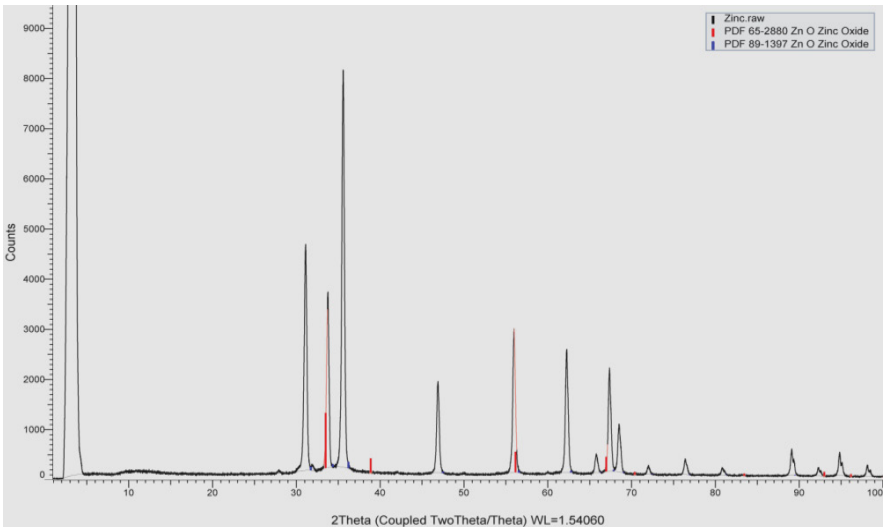

Figure 2: XRD pattern of ZnONPs synthesized at calcining temperatures 500°C

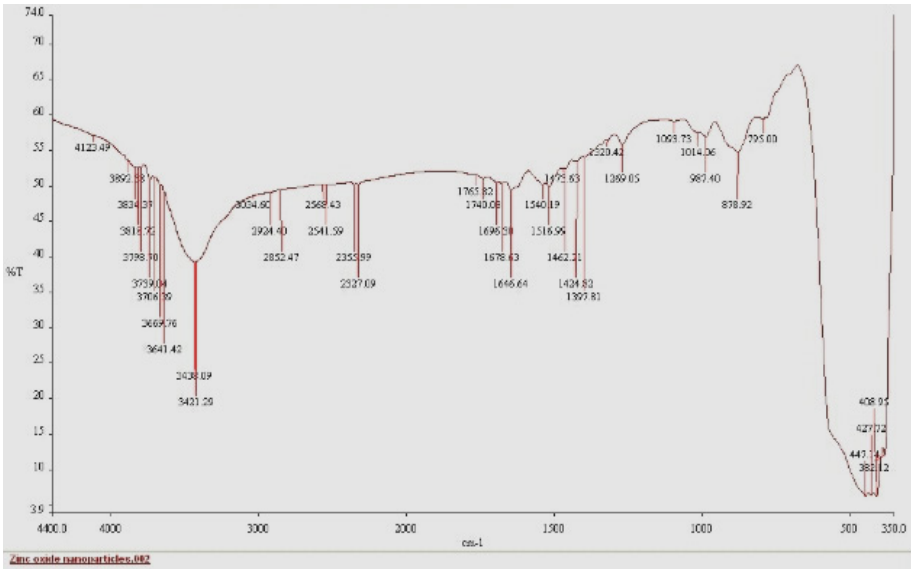

Figure 3: FTIR spectrum of ZnONPs acquired is the range of 400-4000 cm^{-1}

Effect of ZnO-NPs, *Arctium lappa* L. and their combination on the hematological parameters of male rats

Table 1 showed significant ($P \leq 0.05$) decrease in RBCs, Hb, Hct and PLt and a significant ($P \leq 0.05$) increase in WBCs in ZnO-NPs-treated group compared to the control group. In contrast, administration of *Arctium lappa* L. with ZnO-NPs revealed significant ($P \leq 0.05$) increase in RBCs, Hb, Hct and PLt and a significant ($P \leq 0.05$) decrease in WBCs compared to ZnONPs treated group (Table 1).

Table 1: Effect of ZnONPs, *Arctium lappa* L. and their combination on the hematological parameters of male rats

Parameters	Experimental groups			
	Control	ZnO-NPs	ZnO-NPs+*Arctium lappa* L.	*Arctium lappa* L.
RBCs ($\times 10^6$/µl)	8.36 ± 0.04^a	7.40 ± 0.03^b	8.16 ± 0.03^c	8.43 ± 0.05^a
Hb (g/dl)	14.46 ± 0.25^a	12.89 ± 0.26^b	13.60 ± 0.13^c	14.20 ± 0.06^a
Hct (%)	40.70 ± 0.28^a	37.16 ± 0.48^b	38.23 ± 0.47^c	39.83 ± 0.59^a
PLt ($\times 10^3$/µl)	653.50 ± 2.77^a	337.00 ± 0.36^b	543.83 ± 3.39^c	679.00 ± 0.36^a
WBCs ($\times 10^3$/µl)	3.48 ± 0.03^a	5.43 ± 0.04^b	4.26 ± 0.12^c	3.31 ± 0.09^a

Values are expressed as means ± SE; n=7 rats per each group

Mean values within a row not sharing a common superscript letter (a, b and c) were significantly different at $P \leq 0.05$

Effect of ZnO-NPs, *Arctium lappa* L. and their combination on the activities of serum AST, ALT and GGT of male rats

Table 2 revealed significant ($P \leq 0.05$) increases in the activities of AST, ALT and GGT after treatment with ZnO-NPs treated group in respect to the control group. However, administration of *Arctium lappa* L. with ZnO-NPs presented a significant ($P \leq 0.05$) decrease in these enzymes compared to ZnO-NPs treated group (Table 2).

Table 2: Effect of ZnO-NPs, *Arctium lappa* L. and their combination on the activities of serum AST, ALT and GGT of male rats

Parameters	Experimental groups			
	Control	ZnO-NPs	ZnO-NPs+*Arctium lappa* L.	*Arctium lappa* L.
AST (U/L)	45.25 ± 0.73^{a}	82.02 ± 0.58^{b}	45.85 ± 0.47^{c}	42.86 ± 0.54^{a}
ALT (U/L)	31.58 ± 0.26^{a}	55.46 ± 0.43^{b}	32.45 ± 0.36^{c}	31.73 ± 0.56^{a}
GGT (U/L)	43.82 ± 1.33^{a}	54.99 ± 0.44^{b}	47.61 ± 0.51^{c}	41.26 ± 0.36^{a}

Values are expressed as means ± SE; n=7 rats per each group

Mean values within a row not sharing a common superscript letter (a, b and c) were significantly different at $P \leq 0.05$

Effect of ZnO-NPs, *Arctium lappa* L. and their combination on the serum total bilirubin, TP, albumin and globulin of male rats

Chronic ZnO-NPs treatment significantly ($P<0.01$) increased serum total bilirubin while, TP, albumin and globulin were significantly ($P \leq 0.05$) decreased in comparison with the control group (Table 3). While, the oral ingestion of *Arctium lappa* L. with ZnO-NPs caused a significant ($P \leq 0.05$) decrease in the concentration of total bilirubin and significant ($P \leq 0.05$) increase in TP, albumin and globulin as compared to ZnO-NPs-treated group.

Table 3: Effect of ZnO-NPs, *Arctium lappa* L. and their combination on the serum total bilirubin, TP, albumin and globulin of male rats

Parameters	Experimental groups			
	Control	ZnO-NPs	ZnO-NPs+*Arctium lappa* L.	*Arctium lappa* L.
Total bilirubin (mg/dl)	0.27 ± 0.03^{a}	0.41 ± 0.02^{b}	0.31 ± 0.21^{c}	0.25 ± 0.22^{a}
TP (g/dl)	7.60 ± 0.13^{a}	5.51 ± 0.04^{b}	6.30 ± 0.03^{c}	7.60 ± 0.03^{a}
Albumin (g/dl)	2.56 ± 0.02^{a}	1.88 ± 0.22^{b}	2.27 ± 0.05^{c}	2.70 ± 0.03^{a}
Globulin (g/dl)	5.35 ± 0.18^{a}	3.69 ± 0.02^{b}	4.37 ± 0.12^{c}	5.67 ± 0.10^{a}

Values are expressed as means ± SE; n=7 rats per each group .Mean values within a row not sharing a common superscript letter (a, b and c) were significantly different at $P \leq 0.05$

Effect of ZnO-NPs, *Arctium lappa* L. and their combination on the serum total cholesterol, LDL-C, VLDL-C, HDL-C and TG of male rats

The results in Table 4 showed that the oral ingestion of ZnO-NPs caused significant ($P \leq 0.05$) increase in the levels of serum total cholesterol, LDL-C, VLDL-C and TG while, HDL-C was significantly ($P \leq 0.05$) decreased in comparison to the control group. However, the administration of *Arctium lappa* L. with ZnO-NPs showed a significant ($P \leq 0.05$) reduction in the total cholesterol, LDL-C, VLDL-C and TG and a significant ($P \leq 0.05$) elevation in HDL-C compared to ZnO-NPs treated group (Table 4).

Effect of ZnO-NPs, *Arctium lappa* L. and their combination on TBARS, GSH and total thiol in liver and heart of male rats

The data in Table 5 illustrated that the liver and heart TBARS were significantly ($P \leq 0.05$) increased while, GSH and total thiol were significantly ($P \leq 0.05$) decreased in the ZnO-NPs treated group compared to the control group. Moreover, the oral administration of *Arctium lappa* L. with ZnO-NPs showed significant ($P \leq 0.05$) decrease in TBARS and a significant ($P \leq 0.05$) increase in GSH and total thiol compared to ZnO-NPs treated group (Table 5).

Effect of ZnO-NPs, *Arctium lappa* L. and their combination on heart enzymes of male rats

The presented results revealed a significant ($P \leq 0.05$) reduction in the activity of CK-MB and PON1 while, LDH was

Table 4: Effect of ZnO-NPs, *Arctium lappa* L. and their combination on the serum total cholesterol, LDL-C, HDL-C, VLDL-C and TG of male rats

Parameters	Experimental groups			
	Control	ZnO-NPs	ZnO-NPs+*Arctium lappa* L.	*Arctium lappa* L.
Total cholesterol (mg/dl)	94.44 ± 3.08^{a}	131.26 ± 4.01^{b}	90.70 ± 4.04^{c}	92.64 ± 4.10^{a}
LDL-C (mg/dl)	30.53 ± 1.70^{a}	41.59 ± 0.37^{b}	35.07 ± 0.36^{c}	29.71 ± 0.36^{a}
HDL-C (mg/dl)	39.43 ± 0.75^{a}	32.40 ± 0.35^{b}	38.68 ± 0.36^{c}	45.75 ± 0.62^{a}
VLDL-C (mg/dl)	24.48 ± 2.11^{a}	53.27 ± 1.37^{b}	27.95 ± 0.12^{c}	22.18 ± 1.04^{a}
TG (mg/dl)	119.02 ± 0.63^{a}	131.90 ± 2.59^{b}	123.76 ± 1.03^{c}	112.11 ± 3.35^{a}

Values are expressed as means ± SE; n=7 rats per each group. Mean values within a row not sharing a common superscript letter (a, b and c) were significantly different at P ≤ 0.05

Significantly (P ≤ 0.05) increased in ZnO-NPs treated group compared to the control (Table 6). In contrast, supplementation of *Arctium lappa* L. with ZnO-NPs caused significant (P ≤ 0.05) increase in CK-MB, decrease in LDH and PON1 as compared to ZnO-NPs treated group.

Table 5: Effect of ZnO-NPs, *Arctium lappa* L. and their combination on TBARS, GSH and total thiol in liver and heart of male rats

Parameters	Experimental groups			
	Control	ZnO-NPs	ZnO-NPs+*Arctium lappa* L.	*Arctium lappa* L.
Liver				
TBARS (nmol/g tissue)	17.44 ± 0.36^{a}	25.38 ± 0.36^{b}	18.72 ± 0.28^{c}	17.69 ± 0.36^{a}
GSH (µmol/g tissue)	49.18 ± 0.36^{a}	36. 47 ± 0.33^{b}	48.76 ± 0.30^{c}	53.06 ± 0.26^{a}
Total thiol (µmol/g tissue)	8.26 ± 0.06^{a}	4.14 ± 0.11^{b}	5.63 ± 0.08^{c}	8.61 ± 0.03^{a}
Heart				
TBARS (nmol/g tissue)	7.72 ± 0.05^{a}	10.52 ± 0.03^{b}	9.33 ± 0.04^{c}	7.74 ± 0.03^{a}
GSH (µmol/g tissue)	46.53 ± 0.36^{a}	33.12 ± 0.27^{b}	45.71 ± 0.36^{c}	46.8 ± 0.48^{a}
Total thiol (µmol/g tissue)	5.87 ± 0.02^{a}	3.50 ± 0.09^{b}	4.52 ± 0.03^{c}	5.87 ± 0.03^{a}

Values are expressed as means ± SE; n=7 rats per each group. Mean values within a row not sharing a common superscript letter (a, b and c) were significantly different at P ≤ 0.05

Table 6: Effect of ZnO-NPs, *Arctium lappa* L. and their combination on CK-MB, LDH and PON1 of male rats

Parameters	Experimental groups			
	Control	ZnO-NPs	ZnO-NPs+*Arctium lappa* L.	*Arctium lappa* L.
CK-MB (mU/mg protein)	15.41 ± 0.29^{a}	5.08 ± 0.18^{b}	20.45 ± 0.3^{c}	26.57 ± 1.58^{a}
PON1 (U/g protein)	230.6 ± 1.07^{a}	107.3 ± 0.94^{b}	177.6 ± 1.73^{c}	241.0 ± 0.36^{a}
LDH (U/L)	49.54 ± 0.35^{a}	63.27 ± 1.53^{b}	55.2 ± 0.29^{c}	47.82 ± 0.82^{a}

Values are expressed as means ± SE; n=7 rats per each group. Mean values within a row not sharing a common superscript letter (a, b and c) were significantly different at P ≤ 0.05

Effect of ZnO-NPs, *Arctium lappa* L. and their combination on the liver and heart TNF-α, p53 and IL-6 of male rats

The current data in Table 7 showed significant (P ≤ 0.05) increase in TNF-α, p53 and IL-6 in ZnO-NPs treated group in respect to the control group. However, ingestion of *Arctium lappa* L. with ZnO-NPs presented significant (P ≤ 0.05) decrease in TNF-α, p53 and IL-6 as compared to ZnO-NPs treated group (Table 7).

Effects of ZnO-NPs, *Arctium lappa* L. and their combination on the liver and heart ions (Zn^{+2}, Ca^{+2} and Fe^{+2}) of male rats

The rats treated with ZnO-NPs exhibited significant (P ≤ 0.05) elevations in Zn^{+2}, Ca^{+2} and significant (P ≤ 0.05) reduction in Fe^{+2} compared to the control (Table 8). In contrast, the combination of *Arctium lappa* L. with ZnO-NPs led to significant (P<0.05) decrease in Zn^{+2}, Ca^{+2} and significant (P ≤ 0.05) increase in Fe^{+2} as compared to ZnO-NPs

treated group (Table 8).

Table 7: Effect of ZnO-NPs, *Arctium lappa* L. and their combination on the liver and heart TNF-α, p53 and IL-6 of male rats

Parameters	Experimental groups			
	Control	ZnO-NPs	ZnO-NPs+*Arctium lappa* L.	*Arctium lappa* L.
Liver				
TNF-α (pg/ml)	114.62 ± 0.47^{a}	313.13 ± 21.37^{b}	210.96 ± 5.62^{c}	110.42 ± 0.36^{a}
p53 (pg/ml)	5.80 ± 0.03^{a}	14.5 ± 0.36^{b}	7.66 ± 0.12^{c}	4.82 ± 0.08^{a}
IL-6 (pg/ml)	150.07 ± 7.53^{a}	309.46 ± 4.29^{b}	160.92 ± 0.36^{c}	148.51 ± 1.93^{a}
Heart				
TNF-α (pg/ml)	122.77 ± 1.89^{a}	279.62 ± 6.15^{b}	151.93 ± 2.83^{c}	118.73 ± 0.36^{a}
p53 (pg/ml)	5.68 ± 0.15^{a}	10.53 ± 0.47^{b}	7.31 ± 0.15^{c}	5.40 ± 0.03^{a}
IL-6 (pg/ml)	118.07 ± 0.49^{a}	258.74 ± 4.01^{b}	159.20 ± 14.42^{c}	117.48 ± 0.03^{a}

Values are expressed as means ± SE; n=7 rats per each group. Mean values within a row not sharing a common superscript letter (a, b and c) were significantly different at $P \leq 0.05$

Table 8: Effects of ZnO-NPs, *Arctium lappa* L. and their combination on the liver and heart ions (Zn^{+2}, $Ca^{+2}$and Fe^{+2}) in male rats

Parameters	Experimental groups			
	Control	ZnO-NPs	ZnO-NPs+*Arctium lappa* L.	*Arctium lappa* L.
Liver				
Zn^{+2} (µEq/g tissue)	127.73 ± 0.36^{a}	195.50 ± 5.84^{b}	136.19 ± 0.25^{c}	125.39 ± 0.81^{a}
Ca^{+2} (µEq/g tissue)	265.92 ± 0.36^{a}	339.7 ± 4.86^{b}	272.3 ± 0.53^{c}	266.58 ± 12.45^{a}
Fe^{+2} (µg/g tissue)	69.90 ± 1.19^{a}	41.91 ± 1.56^{b}	57.58 ± 4.22^{c}	71.13 ± 0.81^{a}
Heart				
Zn^{+2} (µEq/g tissue)	76.36 ± 1.36^{a}	109.67 ± 1.26^{b}	91.52 ± 1.99^{c}	73.91 ± 1.41^{a}
Ca^{+2} (µEq/g tissue)	450.70 ± 0.36^{a}	512.01 ± 0.32^{b}	486.60 ± 0.36^{c}	448.71 ± 0.36^{a}
Fe^{+2} (µg/g tissue)	20.22 ± 0.13^{a}	12.04 ± 0.40^{b}	17.91 ± 0.20^{c}	21.96 ± 0.49^{a}

Values are expressed as means ± SE; n=7 rats per each group

Mean values within a row not sharing a common superscript letter (a, b and c) were significantly different at $P \leq 0.05$

Histopathological studies

Liver histopathological observations

Liver sections of control rats and *Arctium lappa* L. treated groups showed normal cellular architecture with distinct hepatic cells, sinusoidal spaces and a central vein (Figures 4A and 4D). While, liver of ZnO-NPs-treated group illustrated the histopathological alterations including, distended and hemorrhage in the central and portal veins, degenerated hepatocytes with pyknotic nuclei, hepatocyte vacuolization and dilation of hepatic sinusoids (Figures 4B1 and 4B2). However, liver of rats treated with ZnO-NPs+*Arctium lappa* L. (Figure 4C), revealed that most of the histological changes induced by ZnO-NPs were attenuated from severe to moderate alterations after treatment with *Arctium lappa* L.

Heart histopathological observations

Heart sections of the control and *Arctium lappa* L. treated groups showed normal myofibrillar architecture with striations, branched appearance and continuity with adjacent myofibrils (Figures 5A and 5D). Heart of ZnO-NPs treated group (Figures 5B1 and 5B2) observed loss of normal structure of cardiac muscle fibers, loss of cross striations and fragmentation of sarcoplasm, cytoplasmic vacuolization and degenerative changes in myocardial fibers with dilation and congested blood vessels. Whereas, heart section of *Arctium lappa* L. treated rats showed improvement in

the histopathological changes (Figure 5C).

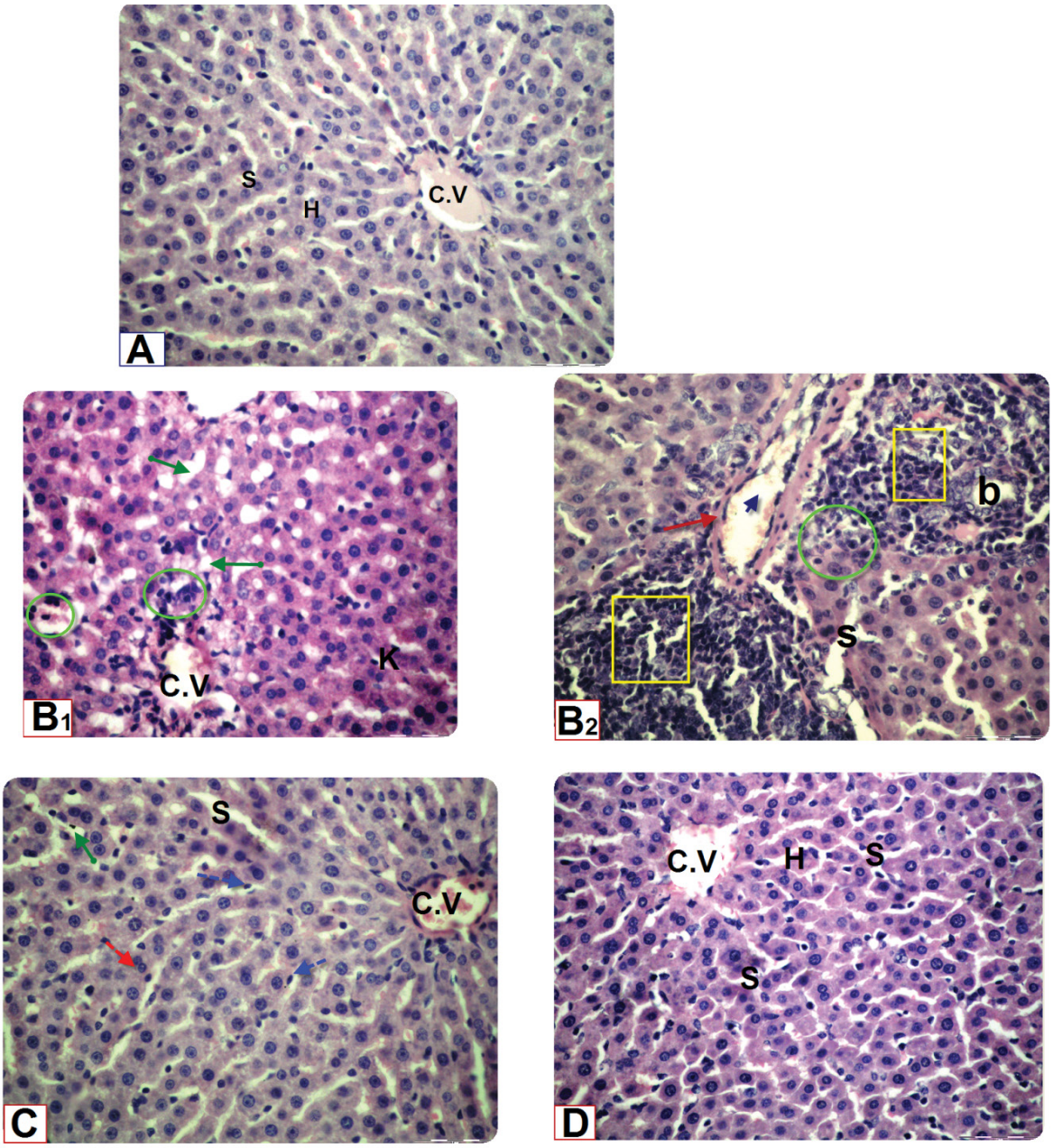

Figure 4: Light micrographs of T.S in the liver tissues of control rat (A) & *Arctium lappa* L.–treated rats (D) showing: normal hepatocytes structure with normal vesiculated nuclei (H), central vein (C.V) and blood sinusoids (s). B1 & B2 T.S in liver of ZnO-NPs-treated rats showing: loss of the normal hepatocyte architecture, fat vacuoles (green arrow), degeneration of hepatocytes (green circle) with pyknotic nuclei, inflammatory infiltrate around portal tract and the bile duct (yellow square & b), dilation and congestion of portal vein (blue head arrow & red arrow). While, liver tissues of ZnO-NPs+*Arctium lappa* L. treated rats (C) showing: mylid improvement in these alterations with the presence of binucleated hepatocytes (red arrow) and few Kupffer cell & vacuoles (blue dotted arrow & green arrow) (H & E stain, x400)

DISCUSSION

The enormous use of ZnO-NPs in the industrial application, it is possible that the human body may be exposed to nanoparticles via several possible routes, including ingestion, inhalation and dermal penetration [30].

In the current study, TEM of ZnO-NPs revealed that, the product consists of spherical particles with the average size of <100 nm which is in close agreement with that estimated by Scherer formula based on the X-Ray Diffraction (XRD) pattern. In addition, the present XRD diffraction lines of ZnO-NPs were broadened dependent on Miller indices of the

corresponding sets of crystal planes. This indicated an asymmetry in the crystallite shape. The crystallite size increases

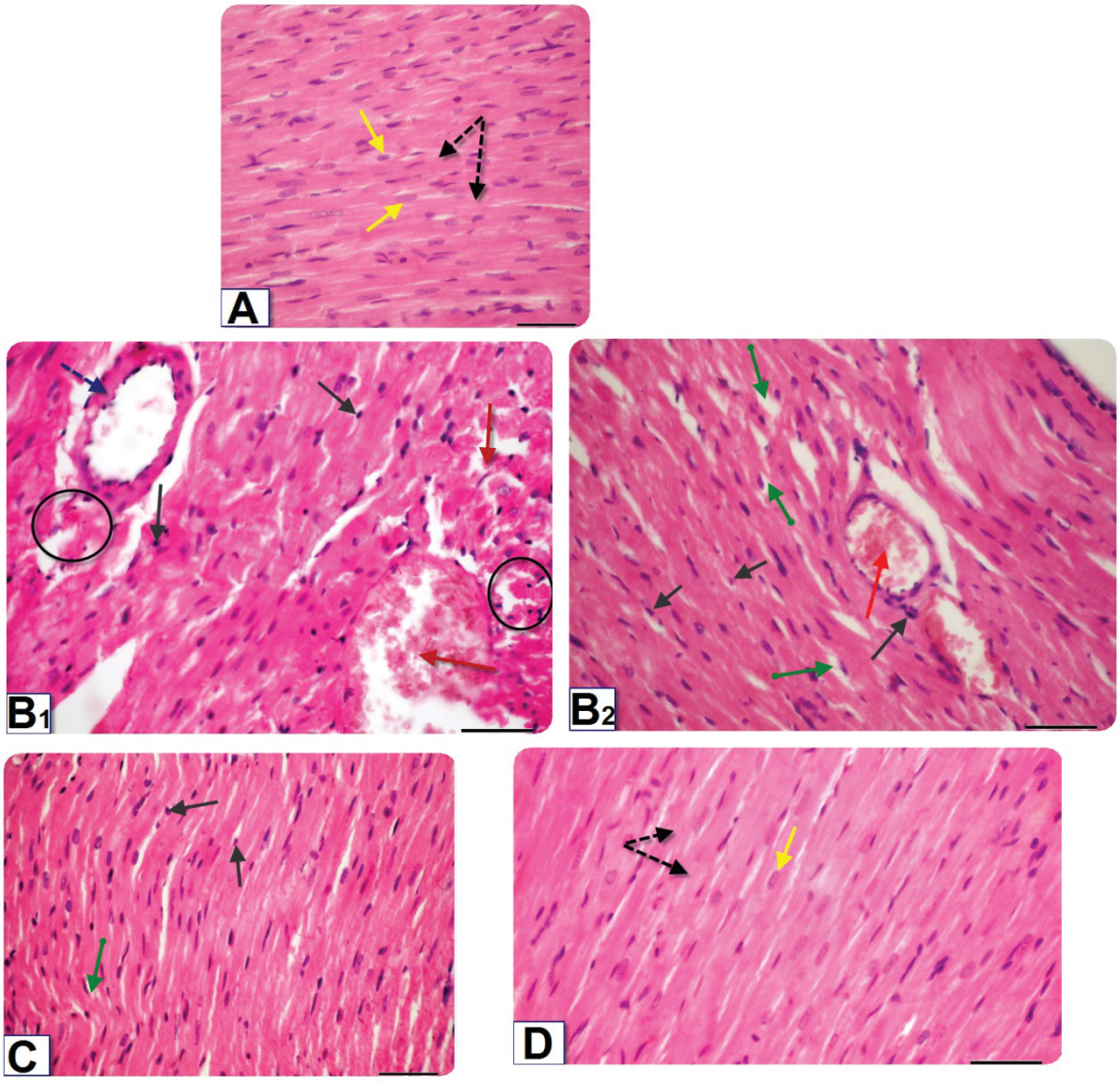

Figure 5: Light micrographs of T.S in the heart tissues of control rat (A) & *Arctium lappa* L. treated rats (D) showing: normal myofibrillar architecture with striations, branched appearance and continuity with adjacent myofibrils and oval nuclei (black dotted arrow & yellow dotted arrow). B1 & B2 heart tissues of ZnO-NPs-treated rats showing loss of normal architecture, disorganization and degeneration in myocardial fibers with pyknotic nuclei (black circle & black arrow), cytoplasmic vacuolization (green arrow) and hemorrhage between myofibrils and blood vessels (red arrow). Also, thickened blood vessel with congestion (blue dotted arrow). While, heart tissues of ZnO-NPs+*Arctium lappa* L. treated rats (C) showing: histological alterations were markedly reduced in the combination group with presence of slight pyknotic nuclei & vacuoles (H & E stain, x400)

slightly by increasing the calcination temperature from 300 to 650°C. The crystallite size of the ZnO-NPs elevated with the rise in calcination temperature [31]. Also, Fang et al. [32] argue that at elevated temperature, the more energy is given to the atoms to prevalent and reside on the adequate site in the crystal lattice and grains with lower surface energy will become larger at elevated temperature. FTIR observed that increasing the annealing temperature sharpens of the distinctive peaks for metal oxide [33].

The anemic status of rats treated with ZnO-NPs might be related to disturbed copper and iron metabolism, resulting in increased intracellular Zn^{2+}, which can cause growth retardation and anemia in animals. These results were consistent with those of Yan et al. [34] who suggested that ZnO-NPs caused significant anemia because of excessive dietary zinc can induce a deficiency in copper and iron. Furthermore, the observed leucocytosis in rats treated with ZnO-NPs,

may be resulted from the inflammatory lesions [35]. However, *Arctium lappa* L. has a curative effect in respect to the alterations in hematological parameters. These results may be attributed to the antioxidant effect of *Arctium lappa* L. by reducing free radical damage [36]. Also, the presence of mucilage in *Arctium lappa* L. which caused a reduction in the levels of total WBCs counts [37].

The present results revealed that ZnO-NPs induced liver damage as documented by the elevations in ALT, AST and GGT, implying cellular leakage and loss of the functional integrity of cell membranes leading to liver dysfunction as reported by Ben-Slama et al. [38]. These enzymes are indicators of the functional efficiency of the liver, and its releasing into the blood reflects the destruction of liver cells [39]. This finding was in agreement with previous reports indicating that sub-acute oral exposure to ZnO-NPs induced hepatocellular necrosis [40]. In addition, the elevations in ALT, AST and GGT were associated with an increase in the plasma membrane permeability of the hepatocyte which, in turn cause cell death [41]. Moreover, administration of ZnO-NPs caused elevation in the levels of total bilirubin and decline in the levels of total protein, albumin and globulin which were compatible with the results of Ko et al. [35]. ZnO-NPs caused oxidative damage to proteins that may lead to enzymatic inactivation and enhance the proteolysis [42]. The reduction in the albumin and the total protein probably describe hepatocellular damage [43]. The hepatoprotective effect of *Arctium lappa* L. may be attributed to its antioxidant effect and free radical scavenging activity as its high levels of flavonoids and polyphenolics thus eliminating the deleterious effects of ZnO-NPs. These results came accordance with Bakr et al. [44] who reported that *Arctium lappa* L. altered the reduction of albumin in diabetic rats. Also, these results may be related to the presence of mucilage, a constituent of *Arctium lappa* L., which increased the levels of total protein, albumin and globulin in hyperlipidemic rats [45].

The present hyperlipidemic effect of ZnO-NPs may be due to the blockage of the liver bile ducts and sign of liver damage, which reduces or stops cholesterol secretion into the duodenum [46]. The hypolipidemia of *Arctium lappa* L. was closely resembling to the results of Wang et al. [47] who stated that *Arctium lappa* L. root extracts reduced the serum total cholesterol, LDL-C and triacylglycerol while, it increased the content of HDL-C in male quails treated with high fat diet. This effect might be related, in part, to its anti-oxidative activity, which decreases the oxidative stress on the hepatocytes, or to other unknown protective mechanism, such as the deflection in the fat accumulation, serum insulin, glucose, insulin resistance [48]. The cholesterol-diminishing activity of *Arctium lappa* L. is mainly in consequence of the reduction of its absorption in the intestinal tract via lowering pancreatic lipase, elevating lipoprotein lipase activity and increase in liver secretion [45].

In the present study, the increased levels of TBARS and decreased glutathione and total thiol in the liver and heart tissues indicated the presence of oxidative stress induced by ZnO-NPs. These findings coincide with Al-Rasheed et al. [49] who reported that ZnO-NPs induced liver damage documented by the elevation in the liver lipid peroxidation and decreased GSH and thiol content. Also, myocardial tissues are susceptible to free radical damage due to fewer amounts of antioxidants like SOD and CAT present in the heart [50]. Also, the present results concomitant with the study of Baky et al. [51] who stated that ZnO-NPs induced cardiotoxicity by elevation in the cardiac injury markers. Watson et al. [52] proved that ZnO-NPs can generate ROS in different ways which are then unavailable to bind other transition metal ions, such as Fe and Cu. These transition metals are then free to catalyze Fenton-type reactions [53]. The anti-oxidative effect of *Arctium lappa* L. may be due to the chemical characterization of *Arctium lappa* L. root studied and found consisting largely of phenolic acid, flavonoid, caffeoylquinic acid and quercetin, these compounds have been proven to possess powerful antioxidant activities [54]. The present results consistent with the results of Cao et al. [55] and Maghsoumi-Norouzabad et al. [56]. Koriem et al. [57] observed depletion in MDA with an increase in the level of GSH in kidney tissue of mice with *Schistosoma haematobium* treated with *Arctium lappa* L. by scavenging ROS and inhibiting the production of further nitric oxide.

The reduction in the activity of CK-MB is an indicator of the severity of ZnO-NPs-induced myocardial damage by destructing myocardial cells [58]. This led to the release of LDH and CK into the blood stream. The amount of these cellular enzymes existent in the blood reflects the modulation in plasma membrane integrity and/or permeability. The izoenzyme PON1 is especially found in endothelial layer of liver, kidneys, heart, brain and testicular tissues. Immunohistochemical methods show that PON1 is also found in smooth muscle cells of aorta as well [59]. Decreased PON1 activity has been reported in various diseases such as diabetes mellitus, atherosclerotic heart disease, rheumatoid arthritis, and chronic renal failure [60]. Results from *in vivo* and *in vitro* basic studies; and from human studies on the association of lower plasma PON1 activity with increased Coronary Artery Disease (CAD) risk [47]. However, the cardio protective effect of *Arctium lappa* L. was parallel to those of Sawant and Bodhankar [61]. They reported that flax lignin which contains arctigenin improved cardiac biomarker CK-MB suggesting that flax lignin offered protection to heart.

The elevation in inflammatory cytokine levels, TNF-α, p53 and IL-6 in rat liver and heart came accordance with Wu et al. [62] and Tang et al. [63]. TNF-α is one of the most commonly inflammatory injurious chemokine immunological markers increased in response to different metal oxide toxicity, including ZnO [64]. It triggers the production of other inflammatory cytokines, including IL-6, the chief stimulator of C-Reactive Protein (CRP) production, leading to inflammatory tissue injury [65]. In addition, the up regurlation of TNF-α, p53 and IL-6 may be due to nanoparticles producing ROS-mediated activation of NF-κB and generation of pro-inflammatory mediators such as TNF-α, IL-8, IL-2 and IL-6 [66]. The elevation in the levels of p53 are in agreement with the recorded results of Setyawati et al. [67] who indicated that apoptotic cell death was induced via the p53 pathway in the presence of high concentration of ZnO-NPs in ROS dependent manner. On the other hand, *Arctium lappa* L. improved liver and heart damage, reduced proinflammatory cytokine levels, and inhibited apoptosis. Song et al. [68] reported that arctigenin treatment partly blocks the increase in IL-6 and TNF-α in the tissue. They suggested that arctigenin suppresses trauma-induced inflammation by inhibiting microglia activation and neutrophil infiltration as well as the release of proinflammatory cytokines, thus, arctigenin exerts anti-inflammatory effects. Arctigenin was reported to possess important pharmacological properties, including anti-tumor, anti-inflammation, immunomodulation, neuroprotection [69]. Arctigenin exhibits anti-inflammatory effects by inhibiting the exudation and recruitment of leukocytes into inflamed tissues via reducing the release/production of inflammatory mediators [70].

The disturbances in the liver and heart Zn^{+2}, Ca^{+2} and Fe^{+2} were consistent with Ben-Slama et al. [38] who reported that ZnO-NPs elevated the concentration of Zn^{+2} and Ca^{+2} in the liver and heart; while, Fe^{+2} was reduced. The elevation in zinc concentration indicates that ZnO-NPs can release zinc ions into cells so that cells can also harbor the NPs simultaneously [71]. Kao et al. [72] hypothesized that the mitochondria sequestered Zn^{+2} released from the ZnO-NPs in the intracellular endosomes, resulting in an increase of mitochondrial zinc concentration, which initiates the apoptotic pathway. Also, Zn^{+2} seem to be responsible for inducing inflammatory responses and necrosis [73]. In addition, the capacity of ZnO-NPs to generate ROS *in vitro* seems to correlate with their potential to induce cellular inflammation *in vivo*. Furthermore, the cardiotoxicity of ZnO-NPs was also coupled with an increase in the cardiac calcium level suggesting alteration in cell calcium homeostasis. This effect may associate with a marked increase in Ca^{+2} permeability [51]. Calcium accumulation in heart cytosol may be a relevant mechanism leading to cell death and has been suggested to play an essential role in the pathogenesis of lethal myocardial cellular injury [74]. *Arctium lappa* L. improved the ions concentration in liver and heart of ZnO-NPs treated rats. These results were in agreement with Scholz et al. [75] and Hussain and Jaccob [76] who confirmed that consumption of flavonoids as a constituent of *Arctium lappa* L. decreased serum and tissue zinc ions to normal values.

The present histological alterations in liver induced by ZnO-NPs go parallel with Saman et al. [30] who reported the liver cells damage, necrosis and lymphocyte infiltration present within the liver tissue after an oral exposure of ZnO-NPs. Once nanoparticles are presented in the cytoplasm, rough grained materials will existent which can cause direct damage and cell death [77]. The hepatoprotective effect of *Arctium lappa* L. can be attributed to its antioxidative role thus eliminating the deleterious effects of toxic metabolites and inducing liver cell regeneration [78]. Moreover, the histological changes in myocardiocytes are in the same line with those reported by EI-Morshedi et al. [79] who observed vacuolar degeneration, necrosis of myocardial cells and separation of the cardiac muscle bundles in the ZnO-NPs treated rats. They indicated that small particles size increases nanoparticle surface area, which stimulate not only the accumulation of nanoparticles in different tissues, but also elevates the reactivity and enhance interactions between nanoparticle and tissue cells. In addition, the histological damage occurred in liver and heart tissues in the ZnO-NPs treated group could be attributed to the inflammation occurred by nanoparticles lead to the generation free radicals which leads to oxidative stress [80]. The current improvement in the myocardial tissue; oval-elongate nucleus and homogeneous cytoplasm in rats treated with *Arctium lappa* L. is compatible with Sawant et al. [61]. They found that flax lignin, which contain arctigenin, treatment showed a decrease in myocardial degeneration and collagen deposition and fibrosis against hypertensive rats.

CONCLUSION

The curative effect of *Arctium lappa* L. could be attributed to a wide range of effective pharmacological compounds, such as polyphenolics, phenolic acid, flavonoid and chlorogenic acid in *Arctium lappa* L., antioxidative and anti-inflammatory effects.

ACKNOWLEDGEMENT

The authors are thankful to the histopathological lab at the High Institute of Public Health, Alexandria University, Egypt the molecular and ; thankful to the molecular and the histopathological lab.

REFERENCES

[1] Huang TC, Tsai SS, Liu LF, Liu YL, Liu HJ, et al. Effect of *Arctium lappa* L. in the dextran sulfate sodium colitis mouse model. *World J Gastroenterol*, **2010**, 16: 4193-4199.

[2] Rasmussen JW, Martinez E, Louka P, Wingett DG. Zinc oxide nanoparticles for selective destruction of tumor cells and potential for drug delivery applications. *Expert Opin Drug Deliv*, **2010**, 7: 1063-1077.

[3] Djurisic AB, Leung YH. Optical properties of ZnO nanostructures. *Small*, **2006**, 2: 944-961.

[4] Teow Y, Asharani PV, Hande MP, Valiyaveettil S. Health impact and safety of engineered nanomaterials. *Chem Comm*, **2011**, 47: 7025-7038.

[5] Koeneman BA, Yang Z, Paul W, Yongsheng C, John C, et al. Toxicity and cellular responses of intestinal cells exposed to titanium dioxide. *Cell Biol Toxicol*, **2010**, 26: 225-238.

[6] Johnston HJ, Hutchison G, Christensen FM, Peters S, Hankin S, et al. A review of the *in vivo* and *in vitro* toxicity of silver and gold particulates: Particle attributes and biological mechanisms responsible for the observed toxicity. *Crit Rev Toxicol*, **2010**, 40: 328-346.

[7] Zhu Z, Yan J, Jiang W, Yao XG, Chen J, et al. Arctigenin effectively ameliorates memory impairment in Alzheimer's disease model mice targeting both β-amyloid production and clearance. *J Neurosci*, **2013**, 33: 13138-13149.

[8] Pasupuleti S, Alapati S, Ganapathy S, Anumolu G, Pully NR, et al. Toxicity of zinc oxide nanoparticles through oral route. *Toxicol Ind Health*, **2012**, 28: 675-686.

[9] Predes FS, Ruiz AL, Carvalho JE, Foglio MA, Dolder H. Antioxidative and *in vitro* anti-proliferative activity of *Arctium lappa* root extracts. *BMC Complement Altern Med*, **2011**, 11: 25-30.

[10] Surye P. Synthesis and characterization of zinc oxide nanoparticles by sol-gel process. National Institute of Technology Rourkela, Orissa, India, **2012**: 1-36.

[11] Bergmeyer HU, Herder M, Red R. Approved recommendation (1985) on IFCC methods for the measurement of catalytic concentration of enzymes, FCC method of alanine aminotransferase. *J Clin Chem Clin Biochem*, **1986**, 24: 481-489.

[12] Szasz G. A kinetic photometric method for serum γ-glutamyl transpeptidase. *Clin Chem*, **1969**, 15: 124-136.

[13] No authors listed. Standardization of methods for measurement of enzymatic activities in biological fluids. *Z Klin Chem Klin Biochem*, **1972**, 10: 182-192.

[14] IFCC. Methods for the measurement of catalytic concentration of enzymes, FICC method for creatine kinase. Japan Information and Culture Center, **1989**, 9: 130-139.

[15] Mueller RF, Hornung S, Furlong CE, Anderson J, Giblett ER, et al. Plasma paraoxonase polymorphism: A new enzyme assay, population, family biochemical and linkage studies. *Am J Hum Genet*, **1983**, 35: 393-408.

[16] Jendrassik L, Grof P. Vereinfachte photometrische methoden zur bestimmung des blutbilirubins. *Biochem Z*, **1938**, 297-299.

[17] Lowry OH, Rosebrough NJ, Farr AL, Randall RJ. Protein measurement with the folin phenol reagent. *J Biol Chem*, **1951**, 193: 265-275.

[18] Doumas BT, Watson WA, Biggs HG. Albumin standards and the measurement of serum albumin with bromcresol green. *Clinica Chimica Acta*, **1971**, 31: 87-96.

[19] Allain CC, Poon LS, Chan CS, Richmond WFPC, Fu PC. Enzymatic determination of total serum cholesterol. *Clin Chem*, **1974**, 20: 470-475.

[20] Assmann G, Jabs HU, Kohnert U, Nolte W, Schriewer H. LDL-cholesterol determination in blood serum following precipitation of LDL with polyvinylsulfate. *Clinica Chimica Acta*, **1984**, 140: 77-83.

[21] Grove TH. Effect of reagent pH on determination of high-density lipoprotein cholesterol by precipitation with sodium phosphotungstate-magnesium. *Clin Chem*, **1979** 25: 560-564.

[22] Bucolo G, David H. Quantitative determination of serum triglycerides by the use of enzymes. *Clin Chem*, **1973**, 19: 476-482.

[23] Tappel AL, Zalkin H. Inhibition of lipid peroxidation in mitochondria by vitamin E. *Arch Biochem Biophys*, **1959**, 80: 333-336.

[24] Jollow DJ, Mitchell JR, Zampaglione NA, Gillette JR. Bromobenzene-induced liver necrosis. Protective role of glutathione and evidence for 3, 4-bromobenzene oxide as the hepatotoxic metabolite. *Pharmacol*, **1974**, 1: 151-169.

[25] Sedlak J, Lindsay RH. Estimation of total, protein-bound and non-protein sulfhydryl groups in tissue with Ellman's reagent. *Anal Biochem*, **1968**, 25: 192-205.

[26] Ferguson-Smith AC, Chen YF, Newman MS, May LT, Sehgal PB, et al. Regional localization of the interferon-β2B-cell stimulatory factor 2/hepatocyte stimulating factor gene to human chromosome. *Genomics*, **1988**, 2: 203-208.

[27] Hedayati M, Yazdanparast R, Azizi F. Determination of human tumor necrosis factor α by a highly sensitive enzyme immunoassay. *Biochem Biophys Res Commun*, **2001**, 289: 295-298.

[28] Hall PA, McCluggage WG. Assessing p53 in clinical contexts: Unlearned lessons and new perspectives. *J Pathol*, **2006**, 208: 1-6.

[29] Drury RAB, Wallington EA. Carleton's histological technique. Oxford University Press, New York, Toronto, **1980**, 237-240.

[30] Saman S, Moradhaseli S, Shokouhian A, Ghorbani M. Histopathological effects of ZnO nanoparticles on liver and heart tissues in wistar rats. *Adv Biores*, **2013**, 4: 83-88.

[31] Kayani ZN, Saleemi F, Batool I. Effect of calcination temperature on the properties of ZnO nanoparticles. *Appl Phys A*, **2015**, 119: 713-720.

[32] Fang ZB, Yan ZJ, Tan YS, Liu XQ, Wang YY. Influence of post-annealing treatment on the structure properties of ZnO films. *Appl Surf Sci*, **2005**, 241: 303-308.

[33] Arafat A, Samad SA, Huq D, Moniruzzaman M, Masum SM. Textile dye removal from wastewater effluents using chitosan-Zno nanocomposite. *J Tex Sci Eng*, **2015**, 5: 1-4.

[34] Yan G, Huang Y, Bu Q, Lv L, Deng P, et al. Zinc oxide nanoparticles cause nephrotoxicity and kidney metabolism alterations in rats. *J Environ Sci Health A*, **2012**, 47: 577-588.

[35] Ko JW, Hong ET, Lee IC, Park SH, Park JI, et al. Evaluation of 2 week repeated oral dose toxicity of 100 nm zinc oxide nanoparticles in rats. *Lab Anim Res*, **2015**, 31: 139-147.

[36] Kucherenko YV, Bernhardt I. Natural antioxidants improve red blood cell "survival" in non-leuko reduced blood samples. *Cell Physiol Biochem*, **2015**, 35: 2055-2068.

[37] Sindhu G, Ratheesh M, Shyni GL, Nambisan B, Helen A. Anti-inflammatory and anti-oxidative effects of mucilage of *Trigonella foenum graecum* (Fenugreek) on adjuvant induced arthritic rats. *Int Immunopharmacol*, **2012**, 12: 205-211.

[38] Ben-Slama I, Mrad I, Rihane N, Mir LE, Sakly M, et al. Sub-acute oral toxicity of zinc oxide nanoparticles in male rats. *J Nanomed Nanotech*, **2015**, 6:1-6.

[39] Aragon G, Younossi ZM. When and how to evaluate mildly elevated liver enzymes in apparently healthy patients. *Cleve Clin J Med*, **2010**, 77: 195-204.

[40] Mansouri E, Khorsandi L, Orazizadeh M, Jozi Z. Dose-dependent hepatotoxicity effects of zinc oxide nanoparticles. *Nanomed*, **2015**, 2: 273-282.

[41] Diab AE, Zahra AA, Al-Dohim MH, Hassan NJ. The impact of *Moringa oleifera* extract and vitamin E against zinc oxide nanoparticles induced hepatotoxicity in male albino rats. *J Am Sci*, **2015**, 11: 85-197.

[42] Parashar A, Badal S. Pomegranate juice is potentially better than orange juice in improving anti-oxidant function in elderly subjects. *Int J Biochem Res Rev*, **2011**, 1: 14-23.

[43] Sodipo OA, Abdulrahman FI, Sandabe UK, Akinniyi JA. Biochemical liver functions with aqueous fruit extract of *Solanum macrocarpum* Linn. in albino rats acutely administered triton-X to induce hyperlipidaemia. *J Appl Pharm Sci*, **2011**, 5: 89-93.

[44] Bakr ESH, ElSawy NA. Therapeutic role of aqueous extract of milk thistle (*Silybum adans* L.) and Burdock (*Arctium lappa*) in hyperglycemic rats. *VRI Bio Med Chem*, **2014**, 2: 20-28.

[45] El-Newary SA, Sulieman AM, El-Attar SR, Sitohy MZ. Hypolipidemic and antioxidant activity of the aqueous extract from the uneaten pulp of the fruit from *Cordia dichotoma. J Nat Med*, **2016**, 70: 539-553.

[46] Kalender S, Uzun FG, Durak D, Demir F, Kalender Y. Malathion-induced hepatotoxicity in rats: The effects of vitamins C and E. *Food Chem Toxicol*, **2010**, 48: 633-638.

[47] Wang Z, Li P, Wang C, Jiang Q, Zhang L, et al. Protective effects of *Arctium lappa* L. root extracts (AREs) on high fat diet induced quail atherosclerosis. *BMC Complement Altern Med*, **2016**, 16: 6-12.

[48] Ahangarpour A, Ali-Akbari FR, Mohaghegh SM, Asadinia E. Effects of *Arctium lappa* aqueous extract on lipid profile and hepatic enzyme levels of sucrose-induced metabolic syndrome in female rats. *Braz J Pharm Sci*, **2016**, 52: 425-431.

[49] Al-Rasheed NM, Fadda LM, Ali HM, Baky NA. Modulation of glutathione, phospholipids and lipid peroxides liver contents induced by zinc oxide nanoparticles using natural antioxidants. *Dig J Nanomater Biostruct*, **2016**, 11: 303-312.

[50] Chennuru A, Saleem MT. Antioxidant, lipid lowering and membrane stabilization effect of sesamol against doxorubicin-induced cardiomyopathy in experimental rats. *Biomed Res Int*, **2013**, 1-5.

[51] Baky NA, Faddah LM, Al-Rasheed NM, Fatani AJ. Induction of inflammation, DNA damage and apoptosis in rat heart after oral exposure to zinc oxide nanoparticles and the cardioprotective role of α-lipoic acid and vitamin E. *Drug Res*, **2013**, 63: 228-236.

[52] Watson CY, Molina RM, Louzada A, Murdaugh KM, Donaghey TC, et al. Effects of zinc oxide nanoparticles on Kupffer cell phagosomal motility, bacterial clearance and liver function. *Int J Nanomed*, **2015**, 10: 4173-4184.

[53] Krężel A, Hao Q, Maret W. The zinc/thiolate redox biochemistry of metallothionein and the control of zinc ion fluctuations in cell signaling. *Arch Biochem Biophys*, **2007**, 463: 188-200.

[54] Ferracane R, Graziani G, Gallo M, Fogliano V, Ritieni A. Metabolic profile of the bioactive compounds of burdock (*Arctium lappa*) seeds, roots and leaves. *J Pharm Biomed Anal*, **2010**, 51: 399-404.

[55] Cao J, Li C, Zhang P, Cao X, Huang T, et al. Anti-diabetic effect of burdock (*Arctium lappa* L.) root ethanolic extract on streptozotocin-induced diabetic rats. *Afr J Biotechnol*, **2012**, 11: 9079-9085.

[56] Maghsoumi-Norouzabad L, Alipoor B, Abed R, Eftekhar Sadat B, Mesgari-Abbasi M, et al. Effects of *Arctium lappa* L. (Burdock) root tea on inflammatory status and oxidative stress in patients with knee osteoarthritis. *Int J Rheum Dis*, **2016**, 19: 255-261.

[57] Koriem KM, Idris ZH, Haron HF, Omar NA, Lazain HS. Therapeutic effect of *Arctium lappa* in *Schistosoma haematobium* associated kidney disturbance: biochemical and molecular effects. *J Parasit Dis*, **2016**, 40: 246-1254.

[58] Nemenqani D. The ameliorating effect of vitamin C against cardiopulmonary toxicity of zinc oxide nanoparticles. *IRJABS*, **2015**, 9: 1102-1109.

[59] Hong-Liang L, De-Pei L, Chihj-Chuan L. Paraoxonase gene polymorphisms, oxidative stress and diseases. *J Mol Med*, **2003**, 81: 766-779.

[60] Goswami B, Tayal D, Gupta N, Mallika V. Paraoxonase: A multifaceted biomoleclue. *Clinica Chimica Acta*, **2009**, 410: 1-12.

[61] Sawant SH, Bodhankar SL. Flax lignan concentrate attenuate hypertension and abnormal left ventricular contractility via modulation of endogenous biomarkers in two-kidney-one-clip (2K1C) hypertensive rats. *Revista Brasileira de Farmacognosia*, **2016**, 26: 601-610.

[62] Wu W, Samet JM, Peden DB, Bromberg PA. Phosphorylation of p65 is required for zinc oxide nanoparticle-induced interleukin 8 expression in human bronchial epithelial cells. *Environ Health Perspect*, **2010**, 118: 982-987.

[63] Tang HQ, Xu M, Rong Q, Jin RW, Liu QJ, et al. The effect of ZnO nanoparticles on liver function in rats. *Int J Nanomed*, **2016**, 11: 4275-4285.

[64] D'Alessandris C, Lauro R, Presta I, Sesti G. C-reactive protein induces phosphorylation of insulin receptor

substrate-1 on Ser307 and Ser612 in L6 myocytes, thereby impairing the insulin signaling pathway that promotes glucose transport. *Diabetologia*, **2007**, 50: 840-849.

[65] Kerner A, Avizohar O, Sella R, Bartha P, Zinder O, et al. Association between elevated liver enzymes and C-reactive protein. *Arterioscler Thromb Vasc Biol*, **2005**, 25: 193-197.

[66] Byrne JD, Baugh JA. The significance of nanoparticles in particle-induced pulmonary fibrosis. *Mcgill J Med*, **2008**, 11: 43.

[67] Setyawati MI, Tay CY, Leong DT. Effect of zinc oxide nano-materials-induced oxidative stress on the p53 pathway. *Biomaterials*, **2013**, 34: 10133-10142.

[68] Song J, Li N, Xia Y, Gao Z, Zou SF, et al. Arctigenin treatment protects against brain damage through an anti-inflammatory and anti-apoptotic mechanism after needle insertion. *Front Pharmacol*, **2016**, 7: 182-198.

[69] Swarup V, Ghosh J, Mishra MK, Basu A. Novel strategy for treatment of Japanese encephalitis using arctigenin, a plant lignan. *J Antimicrob Chemother*, **2008**, 61: 679-688.

[70] Zhang N, Wen Q, Ren L, Liang W, Xia Y, et al. Neuroprotective effect of arctigenin via upregulation of P-CREB in mouse primary neurons and human SH-SY5Y neuroblastoma cells. *Int J Mol Sci*, **2013**, 14: 18657-18669.

[71] Amara S, Slama IB, Mrad I, Rihane N, Khemissi W, et al. Effects of zinc oxide nanoparticles and/or zinc chloride on biochemical parameters and mineral levels in rat liver and kidney. *Hum Exp Toxicol*, **2014**, 33: 1150-1157.

[72] Kao YY, Chen YC, Cheng TJ, Chiung YM, Liu PS. Zinc oxide nanoparticles interfere with zinc ion homeostasis to cause cytotoxicity. *Toxicol Sci*, **2012**, 125: 462-472.

[73] Landsiedel R, Ma-Hock L, Kroll A, Hahn D, Schnekenburger J, et al. Testing metal-oxide nano-materials for human safety. *Adv Mater*, **2010**, 22: 2601-2627.

[74] Kain V, Kumar S, Sitasawad SL. Azelnidipine prevents cardiac dysfunction in streptozotocin-diabetic rats by reducing intracellular calcium accumulation, oxidative stress and apoptosis. *Cardiovasc Diabetol*, **2011**, 10: 1-97.

[75] Scholz E, Zitron E, Katus HA, Karle CA. Cardiovascular ion channels as a molecular target of flavonoids. *Cardiovasc Ther*, **2010**, 28: e46-e52.

[76] Hussain SA, Jaccob AA. Effects of single oral doses of flavonoids on absorption and tissue distribution of orally administered doses of trace elements in rats. *Am J Pharmacol Sci*, **2013** 1: 84-89.

[77] Su YK, Peng SM, Ji LW, Wu CZ, Cheng WB, et al. Ultraviolet ZnO nanorod photosensors. *Langmuir*, **2009**, 26: 603-606.

[78] Lin SC, Lin CH, Lin CC, Lin YH, Chen CF, et al. Hepatoprotective effects of *Arctium lappa* Linne. on liver injuries induced by chronic ethanol consumption and potentiated by carbon tetrachloride. *J Biomed Sci*, **2002**, 9: 401-409.

[79] EI-Morshedi N, AlZahrani I, Kizibash NA, Al-Fayez HAA. Toxic effect of zinc oxide nanoparticles on some organs in experimental male *Wistar* rats. *Int J Adv Res*, **2014**, 2: 907-915.

[80] Kreyling WG, Semmler-Behnke M, Möller W. Health implications of nanoparticles. *J Nanopart Res*, **2006**, 8: 543-562.